

NASA REDUCED GRAVITY STUDENT FLIGHT
OPPORTUNITIES PROGRAM PROPOSAL
SPRING 1999 COMPETITION

AN EXPERIMENTAL STUDY OF NATURAL
CONVECTION IN ARTIFICIAL GRAVITY



SUBMITTED BY THE FOLLOWING TEAM MEMBERS:

MICHAEL H. BELL/ MECHANICAL ENGINEERING/ SENIOR
TEQUILA GRIGGS/ MECHANICAL ENGINEERING/ SENIOR
JARRID LATTA/ MECHANICAL ENGINEERING/ SENIOR
ALICE NELMS/ MECHANICAL ENGINEERING/ SENIOR
RICHARD SHUNNARAH/ MECHANICAL ENGINEERING/ SENIOR
DAMON SPARKS/ MECHANICAL ENGINEERING/ SENIOR
GEORGE XENOFOS/ MECHANICAL ENGINEERING/ SENIOR
MICHAEL ZARICHNAK/ MECHANICAL ENGINEERING/ SENIOR

POINT OF CONTACT – MICHAEL H. BELL / bellm@eng.uab.edu / 205-647-4949

FACULTY ADVISOR – PROFESSOR JOHN BAKER / jbaker@eng.uab.edu / 205-934-7508

RETURN TO:
MICHAEL H. BELL
DEPARTMENT OF MATERIALS AND MECHANICAL ENGINEERING
UNIVERSITY OF ALABAMA AT BIRMINGHAM
1150 10TH AVENUE SOUTH
BIRMINGHAM, AL 35294-4461

SUBMITTED TO:

NASA REDUCED GRAVITY STUDENT FLIGHT OPPORTUNITIES
ATTN: MR. BURKE O. FORT
TEXAS SPACE GRANT CONSORTIUM
3925 WEST BRAKER LANE, SUITE 200
AUSTIN, TEXAS 78759-5321

ABSTRACT

This proposal outlines an experimental investigation of natural convection in a rectangular enclosure with the presence of a non-uniform artificial gravity field. The non-uniformity in the artificial gravity field occurs as a result of the fact that centrifugal forces produce the artificial gravity field and such forces are proportional to the distance from the axis of rotation. Recall that natural convection depends upon buoyancy forces and buoyancy forces are proportional to gravitational acceleration. Conducting the experiment on the KC-135 will eliminate terrestrial gravitational acceleration and the associated buoyancy forces. This will allow student investigators to examine natural convection that is purely the result of the buoyancy forces associated with the artificial gravity field.

A fully enclosed experimental test cell has been designed. The test cell contains power supplies, an accelerometer, a fully instrumented enclosure along with thermoelectric devices for heating and cooling the “top” and “bottom” walls, a data acquisition system, and a computer. An external motor fixed to a frame that houses the entire experiment will be used to rotate the test cell. Rotational speed will be measured using an optical tachometer.

The overall objective of the proposed experiment is to develop a basic understanding of natural convection in a rotationally produced artificial gravity field. The specific aims of the proposed experiment are:

- 1) Conduct a series of experiments focusing on natural convection in an artificial gravity field.
- 2) Perform a parametric investigation to determine natural convection characteristics in an artificial gravity.
- 3) Use the information gained from the parametric investigation to develop Nusselt number correlations for natural convection in an artificial gravity.

In addition to the above specific aims, an outreach program will be developed as part of the overall project. The outreach program will: 1) provide information about project activities and 2) promote the human exploration and development of space to the general public.

The proposed research is motivated by the fact that continued exposure to a microgravity environment is known to produce a number of undesirable physiological effects in humans. For a long-duration space flight, such as a manned mission to Mars, changes in human physiology caused by weightlessness could detrimentally affect the success of such a mission. For a spacecraft that employs an artificial gravity, accounting for buoyancy force interactions will be critical to the design of systems such as life support or fire protection.

TABLE OF CONTENTS

1. INTRODUCTION	1
1.1 OVERVIEW	1
1.2 THEORY	3
2. TEST EQUIPMENT DATA PACKAGE.....	5
2.1 Synopsis.....	5
2.2 Test Objectives.....	6
2.3 Test Description.....	6
2.4 Equipment Description.....	7
2.5 Structural Load Analysis	10
2.6 Electrical Load Analysis.....	11
2.7 Pressure Vessel Certification.....	11
2.8 Flight Test Procedures.....	12
2.9 Parabola Requirements.....	13
2.10 Ground Support.....	13
2.11 Flight Support	13
2.12 Data Acquisition System	13
2.13 Test Operating Limits or Restrictions.....	13
2.14 Flight Manifest.....	14
2.15 Photographic Requirements.....	14
2.16 Hazard Analysis	15
3. OUTREACH PLAN	17
4. PROJECT BUDGET.....	18
5. PERSONAL LIFE ACCIDENT INSURANCE	19
6. REFERENCES	20
APPENDIX A – SAMPLE CALCULATIONS.....	21
APPENDIX B – UNCERTAINTY ANALYSIS	23
APPENDIX C – AGE VERIFICATION.....	26
APPENDIX D – FACULTY ENDORSEMENT	27
APPENDIX E – TEAM ADVISOR.....	28

1. INTRODUCTION

1.1 Overview

As space exploration increases, longer periods of time will be spent in a microgravity environment. Unfortunately, long-term exposure to weightlessness leads to a chain-reaction of undesirable physiological adaptations. Among these are bone demineralization, cardiovascular changes, fluid redistribution, and red blood cell loss. In order to solve these problems, experiments and studies must be conducted. There is both theoretical and experimental evidence that artificial gravity can substitute for natural gravity to maintain health in orbit.

An experiment studying natural convection in an artificial gravity has practical application in space habitat design. In order to counteract the effects of microgravity on the human body, space habitats may use centrifugal force to create an artificial gravity. This artificial gravity will vary as the distance from the center changes, resulting in a non-uniform gravity field. Because natural convection heat transfer is affected by the magnitude of the gravity field, design of spacecraft life support systems will depend upon an understanding of natural convection in an artificial gravity field. By understanding how the heat is transported, optimal placement, size, and power consumption of heating and cooling equipment can be assessed. Minimization of size, weight, and power consumption leads to more cost-effective space flights.

In this experiment, an experimental test cell will be used to determine natural convection heat transfer characteristics in an artificial gravity field. The test cell is placed at a given radius from the center of rotation as shown in figure 1.

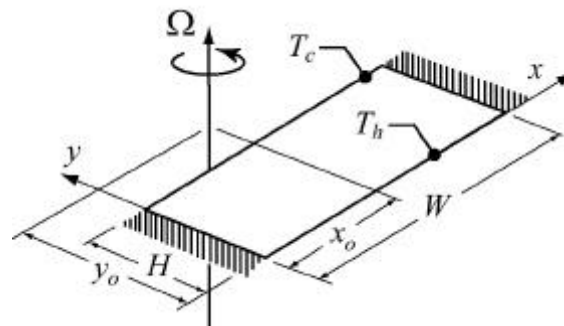


Figure 1: Diagram of Test Cell in Relation with Axis of Rotation

Rotating the enclosure about an axis will generate an artificial gravity field. A thermoelectric device is positioned at the outer edge of the test cell and a heat sink is positioned at the inner edge. When the external gravitational acceleration due to the flight path of the KC-135 becomes less than 1-g, heat is transferred into one end of the test cell while a heat sink at the opposite end draws this heat to maintain isothermal conditions at the two walls. Note that the other walls of the test cell are insulated. The test cell will be instrumented with thermistors placed within the test cell walls. The information from the test cell will be routed to a computer system equipped with a data acquisition system as shown in figure 2. The experimental test cell will be enclosed in a PVC cylinder and will be isolated from the surroundings. The PVC cylinder will be housed in a frame and will be rotated using an external, variable speed motor. Temperatures, rotational speeds, and external gravitational acceleration will be measured. This information will be used to determine convective instability and to examine the validity of certain scaling arguments.

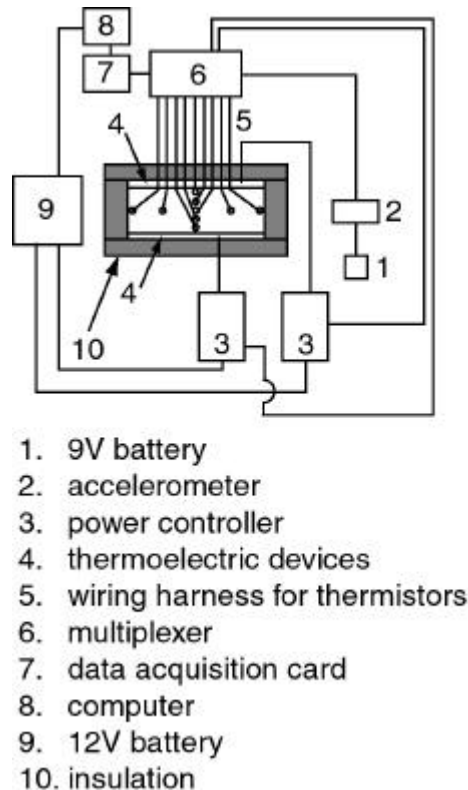


Figure 2: Schematic of Test Cell and Data Acquisition System

1.2 THEORY

The phenomenon of natural convection heat transfer plays an important role, both in nature and in engineering systems (Kakac 1985). In natural convection, fluid motion is the result of buoyancy forces. The ratio of the buoyant forces to viscous forces, a dimensionless number known as the Grashof number, can be used to predict the onset of natural convection. For an enclosure, a dimensionless parameter, known as the Rayleigh number, has traditionally been used. The Rayleigh number is the product of the Grashof number and the Prandtl number. The Prandtl number is the ratio of the viscous forces to thermal diffusivity. Previous research has identified a critical value of the Rayleigh number. Below this critical value the only mode of heat transfer is by conduction. Above this critical value natural convection occurs (Holman 1997).

Gravity is minimal in space, therefore, natural convection as a result of density gradients can not occur. As mentioned in the introduction section there is a critical need to provide an artificial gravity environment for a long duration space flight. Currently, the only known method of producing such an environment is by rotating a spacecraft. Artificial gravity is produced as a result of centrifugal forces.

On earth the gravitational acceleration is a constant and is approximately equal to 9.81 m/s^2 . In this artificial gravity environment, the gravitational acceleration will not be constant. The artificial gravity acceleration will be a monotone increasing function of the distance from the axis of rotation. The equation for the artificial gravitational acceleration is $a = \Omega^2 \cdot r$, where r (meters) is the distance from the axis of rotation and Ω (radians per second) is the angular speed. To achieve Earth-normal gravity, the required distance from the axis of rotation is a function of rotational speed, which is shown in figure 3.

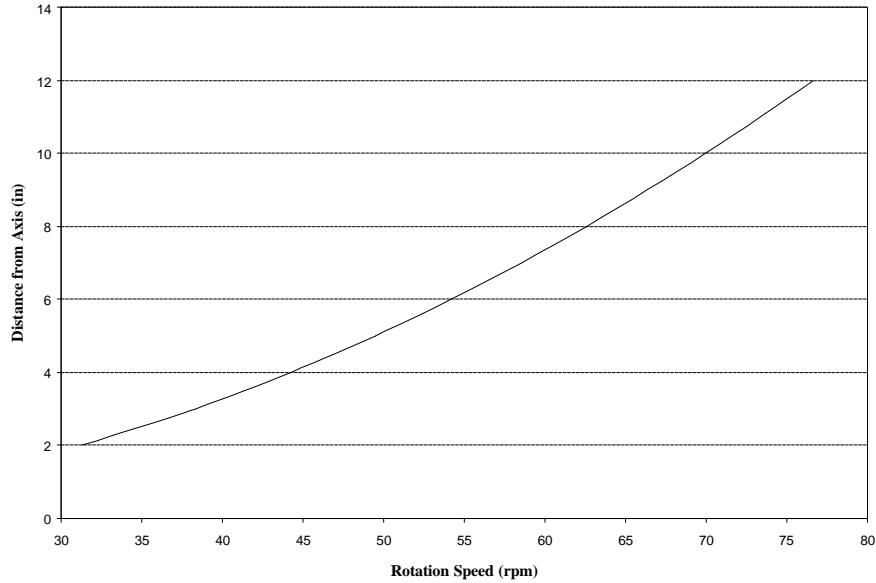


Figure 3: Distance from Axis vs. Rotational Speed for 1-g

In this investigation natural convection in a rotating enclosure will be considered. After examining the problem, it was decided that the following variables will be important in predicting natural convection characteristics: ΔT , q_w , Ω , H , W , β , μ , k , ρ , c_p . ΔT is the change in temperature, q_w is the wall heat flux, Ω is the angular velocity, H is the height, W is the width, β is the coefficient of thermal expansion, μ is the viscosity, k is the thermal conductivity, ρ is the density, c_p is the specific heat at constant pressure. These variables were used to derive three dimensionless parameters. These parameters are the Prandtl Number, Nusselt Number, and an unknown, N_2 . N_2 was derived by applying the Buckingham-Pi theorem (Baker-Nayagam 1999).

As part of the planning phase of the experiment, an uncertainty analysis was performed to determine the most cost-effective means of accurately measuring each variable. The uncertainty analysis was performed for RTD's, thermistors, and thermocouples. From the analysis of our results, thermistors were proven to be the most cost-effective and precise. See appendix B for uncertainty analysis.

2. TEST EQUIPMENT DATA PACKAGE

2.1 Synopsis

In this experiment, characteristics of natural convection will be examined in a non-uniform artificial gravity field. Design of spacecraft life support systems will depend upon an understanding of natural convection in an artificial gravity field because natural convection heat transfer is affected by the magnitude of the gravity field. Rotating the test cell about an axis will provide an artificial gravity field. The test cell will be heated at one end and cooled at the other. Temperatures, rotational speeds, and gravitational acceleration will be measured. This information will be used to determine convective instability and to examine the validity of certain scaling arguments.

2.2 Test Objectives

The objectives of this experiment are the following:

- Conduct an experiment capable of exploring natural convection in an artificial gravity field.
- Conduct a parametric investigation on the onset of the initial convective instability. The parameters that are varied are the change in temperature across an enclosure and rotational speed. Develop a neutral stability curve for the onset of the initial convective instability.
- Gain insight into natural convection in an artificial gravity field and develop a correlation of natural convection heat transfer characteristics in an artificial gravity field.

2.3 Test Description

Flight onboard the KC-135A will provide gravitational accelerations varying from microgravity to 2-g during parabolic flight maneuvers. A test cell, within a rotating PVC cylinder will be heated at one end and cooled at the other. Temperatures, rotational speeds, and gravitational acceleration will be measured continuously by a data acquisition system. The data acquisition will control the thermoelectric devices.

2.4 Equipment Description

Structure

A structure will be constructed of T-slotted extruded aluminum struts. The dimensions of the structure will be 24 inches by 24 inches by 48 inches. Bolts will connect the struts. The structure will be mounted to an aluminum base plate. The struts, bolts, and connectors are manufactured by 80/20, Inc.

Base plate

An aluminum base, with dimensions of 24 inches by 48 inches and ¼-inch thick, will be attached to the floor of the KC-135 with 5/8-inch steel bolts. The bolts will be protected with large area washers according to the specifications given in the Student Flight Opportunities User guide.

Cylinder

A PVC cylinder will have an inside diameter of 10-inches and a length of 48-inches. Aluminum caps on both ends will enclose the cylinder. The caps will be secured to the cylinder by threaded rods travelling inside the length of the cylinder bolted to each cap. The cylinder will serve as the housing for a rail cage that will house the test cell, data acquisition system, and a 12-volt battery.

Motor

The motor will be a Dayton 4Z248 ¼-hp, variable speed, AC motor. The motor's maximum rpm is 1725 rpm.

Tachometer

A Cole-Parmer optical tachometer will be used to measure rotational speeds. The model number is P-87303-10.

Surge protector

The surge protector will be a standard 6-plug extension surge bar. This will be used to provide 120-volts AC for the motor.

Batteries

Two gel-cell batteries will supply power to the PC/104 computer, the thermoelectric devices, and thermistors. A 9-volt battery will supply power to the accelerometer.

Data acquisition card

The data acquisition board will provide the PC/104 data it reads from the thermocouples and accelerometer. This data acquisition board will sit next to the laptop computer and will be connected to the thermocouples and accelerometer. We are planning to purchase this equipment from National Instruments.

Multiplexer

The AMUX-64T is a front-end analog multiplexer that quadruples the number of analog input signals that can be digitized with National Instruments MIO board. Thermistors will be connected to the AMUX-64T and the AMUX-64T will be connected to the data acquisition card. The AMUX-64T has 16 separate four-to-one analog multiplexer circuits. The AMUX-64T has an integrated circuit temperature sensor that can be connected as a differential input of two of the 64 input channels for thermistor cold-junction compensation.

Computer

The Parvus PC/104 single board computer will be used to operate LabVIEW, which will collect data from the data acquisition card and operate the thermoelectric device. The PC/104 utilizes a credit-card-size Pentium processor. The footprint of the PC/104 is 3.55-inches by 3.775-inches. The PC/104 will receive its power from the Parvus Power Distribution IV, which is a DC to DC conversion board. The Power Distribution IV will receive its power from batteries.

Thermistors

Omega ON-402-PP thermistors will be used to record temperatures in the walls of the test cell. The ON-402-PP has a temperature range of 32° F (0°C) to 212°F (100°C).

Accelerometer

An 8352A K-BEAM Capacitive Accelerometer Module will be used to measure gravitational acceleration of the KC-135. The Kistler 8352A2 accelerometer has an

acceleration range of $\pm 2g$ and a sensitivity of 500 mV/g. This accelerometer will be connected to the data acquisition board.

Test cell

Teflon will be the primary material of the test cell. The test cell is a rectangular enclosure with a hollow cavity. There will be a heater at one end and a heat sink at the opposite end. It will be sealed at each end with o-rings and aluminum plates connected with threaded rods. Holes, drilled into the walls of the test cell, will be instrumented with thermistors.

Heater

Melcor's model CP 2-127-10L thermoelectric module will provide the heat for the test cell. Batteries will supply its power and will be controlled by LabVIEW.

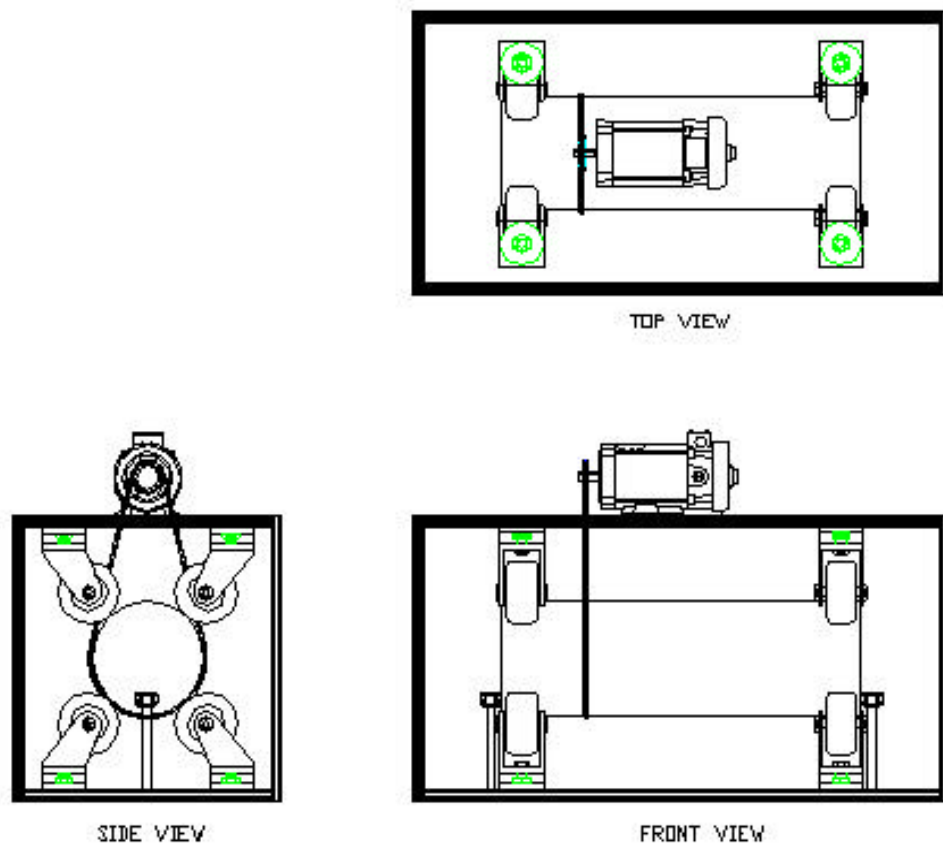


Figure 4: Test Structure Schematic

2.5 Structural Load Analysis

Shear Stress

		Base Plate		Acrylic Lid		
# of g's	Shear Force (lbs)	Bolt Area (in ²)	Shear Stress (psi)	Shear Force (lbs)	Bolt Area (in ²)	Shear Stress (psi)
0	0.00	0.11045	0.00	0.00	0.02761	0.00
1	16.32	0.11045	147.75	0.21599	0.02761	7.82
2	32.64	0.11045	295.50	0.43197	0.02761	15.64
3	48.95	0.11045	443.24	0.64796	0.02761	23.47
4	65.27	0.11045	590.99	0.86394	0.02761	31.29

Weight

# of g's	PVC Cylinder (lbs)	Aluminum Frame (lbs)	Computer (lbs)	Teflon (lbs)	Cylinder Lids (lbs)	Total (lbs)
0	0	0	0	0	0	0
1	30.128	17.82	10	4.733	2.592	65.273
2	60.256	35.64	20	9.466	5.184	130.546
3	90.384	53.46	30	14.199	7.775	195.819
4	120.512	71.28	40	18.932	10.367	261.092

Structural Properties

# of g's	Maximum Deflection		Allowable Stress (psi)	Tensile Strength (psi)	Max. Allowable Load	
	Long Beams (in)	Short Beams (in)			Compression Force (lbs)	Tension Force (lbs)
0	0	0	N/A	N/A	N/A	N/A
1	0.0016582	0.0002073	35000	38000	15225	16530
2	0.0033165	0.0004146	17500	19000	7612.5	8265
3	0.0049747	0.0006218	11667	12667	5075	5510
4	0.0066329	0.0008291	8750	9500	3806.25	4132.5

Rotation Speed for Cylinder

# of g's	Radius (in)	Radius (ft)	W (rad/s)	W (RPM)
0	5	0.417	0	0
1	5	0.417	8.791	83.947
2	5	0.417	12.432	118.719
3	5	0.417	15.226	145.400
4	5	0.417	17.582	167.894

Pulley Size

# of g's	Diameter (in)	W (RPM)	Diameter (in)	W (RPM)	Diameter (in)	W (RPM)
0	0.5	0	1	0	2	0
1	0.5	1678.94	1	839	2	420
2	0.5	2374.38	1	1187	2	594
3	0.5	2908.01	1	1454	2	727
4	0.5	3357.88	1	1679	2	839

2.6 Electrical Load Analysis

During the flight, the motor will draw from the aircraft electrical test power. Other components of the project will draw its power from a series of batteries. All components of the project are UL certified products. The following in-flight maximum electrical power requirements are summarized in table 1:

Item	Volts	Amps (approx.)	Hz
Motor (KC-135A)	110	4.2	60 Hz AC
Thermistor (battery)	2	625 mA	N/A
Computer (battery)	12	5 mA	N/A
Heater (battery)	8.6	9	N/A
Accelerometer (battery)	9	8 mA	N/A

Table 1: Maximum Power Requirements

2.7 Pressure Vessel Certification

Not applicable

2.8 Flight Test Procedures

Pre-Boarding Checklist	
Task	Check
Verify rounded corners and padding on edges	
Check all connections	
Check computer	
Check motor	
Verify all systems operate properly	
Verify LabVIEW runs properly	
Test thermistors	

Post Boarding—Pre-flight Check	
Task	Check
Base plate secured	
Computer turned off and secured	
All hardware secured	

In-Flight—Experimental Setup	
Task	Check
Turn on computer	
Access data acquisition program	

Perform Experiment	
Task	Check
Initiate data acquisition	
Seal cylinder	
Secure bearings	
Turn on motor	

Post Experiment—Before Landing	
Task	Check
Turn off motor	
Turn off computer and secure all hardware	

2.9 Parabola Requirements

This experiment requires 10 parabolas, minimum, per flight.

2.10 Ground Support

For a given flight day, the flight crewmembers that are not flying that day will serve as the ground crew. Their responsibility is ensuring that the batteries are fully charged.

2.11 Flight Support

The interfaces to the KC-135 that are necessary for this experiment are the area to which we attach our base plate and a power source.

2.12 Data Acquisition System

The PC/104 computer will have National Instrument's LabVIEW installed and will be programmed to measure and collect the variables necessary to determine the onset of natural convection. LabVIEW is a development environment based on the graphical programming language G. Programs in LabVIEW are known as VIs, or virtual instruments. The VI written for this project will have the following instructions:

- Measure the gravitational acceleration onboard the KC-135 from accelerometer
- When gravitational acceleration decreases below a certain predetermined value, turn on thermoelectric devices
- Measure and record temperature readings from thermistors
- When gravitational acceleration increases above a certain predetermined value, turn off the heating thermoelectric device. The cooling thermoelectric device will ensure that the temperature in the enclosure at the beginning of each run is the same.
- Repeat for each parabola.

2.13 Test Operating Limits or Restrictions

There are not any limits or restrictions regarding this experiment.

2.14 Flight Manifest

Flight Day 1:

Personnel – Michael Bell and Jarrid Latta

Flight Day 2:

Personnel – Richard Shunnarah and George Xenofos

2.15 Photographic Requirements

This experiment does not require any photography, however, video and photographic support is requested for outreach purposes.

2.16 Hazard Analysis

Hazard 1: Electrical Fire

Description: Fire outbreak in electrical system.
Causes: Potential fire outbreak due to faulty electrical wiring.
Control: All wiring will be properly and correctly connected. Electrical tape will be used to aid in this purpose.
Verification: Wiring will be inspected prior to flight to verify connection

Hazard 2: Electrical Shock

Description: Shock and potential injury from electrical wiring.
Causes: Contact with exposed wiring cause electrical shock during experimentation.
Control: All wires will be properly insulated. A wire nut will be used at all connections (where feasible). Electrical tape will be used where necessary.
Verification: Inspection of all connections and wires prior to flight

Hazard 3: Cuts From Sharp Edges on Support Frame

Description: Injury due to sharp edges on support frame.
Cause: Collision with sharp edges.
Control: Rounding of corners (where feasible and if strength of material is not jeopardized) or padding.
Verification: Inspection of edges prior to flight

Hazard 4: Exploding Batteries

Description: Recharging batters have been known to explode.
Causes: Overcharging batteries may cause the batteries to explode.
Control: Only new batteries will be used.
Verification: Manufacturer's certification

Hazard 5: Structural Failure

Description: Failure of the structure during experimentation.
Cause: Structure is under-designed and fails during flight due to the 9-g acceleration.
Control: Both structures will be properly designed to withstand the expected load.
Verification: Structures will be analyzed through mathematical and experimental means.

Hazard 6: Injury Resulting From Flying Objects

Description: Injury from flying objects such as sample pieces.
Cause: Injury will be due to: pieces may break during rotation and become projectiles, causing injury upon impact.
Control: Injury will be prevented by: Total enclosure of components to prevent flying objects from colliding with equipment or people.
Verification: Inspection of structure to verify complete enclosure

3. OUTREACH PLAN

Our outreach program has been designed to enlighten the general public about the scientific aspects of the project. Exposure of our experiences may encourage students to the areas of physical sciences and engineering. Furthermore, the results of this project will be available for those interested in the characteristics of natural convection in artificial gravity.

From Birmingham's Fox TV affiliate, reporter Rick Journey will be onboard the plane during the experiment. His role in this project will be to document and report the experience of the flight. Also, The McWane center, a museum that specifically focuses on science related fields has offered time slots so that we may exhibit our project to the public.

A web-site will be created that presents the details of the experiment and our experiences in the NASA Reduced Gravity Student Flight Opportunities program. The website will contain:

- information such as photographs of the actual flight
- AVI files of video from the flight, and
- personal comments about what it feels like to experience microgravity

In order to share our experience the team members will be visiting local school systems. The team intends to show students that science is challenging and at the same time fun. Perhaps from this, these young students may find a new fascination for the area of space exploration.

Every year the School of Engineering at the University of Alabama at Birmingham holds an open house for the general public and high school students in Alabama who are interested in learning more about opportunities for careers in engineering. The team members plan to bring the results of their work to the next Open House through a multi-media presentation, video clips from the flight, and a brief summary of results to show the type of work that undergraduate students can do.

5. Personal Accident Life Insurance

The Boeing KC-135A is a four-engine, swept-wing aircraft similar to the Boeing 707. KC-135's are primarily operated by USAF as a refueling tankers; however this particular KC-135A, NASA 931, which was obtained by NASA in November of 1994, has been modified by NASA to support the Reduced Gravity Program. The predecessor to NASA 931, NASA 930 was obtained by NASA in 1973 and flew over 58,000 parabolas before being retired in 1995.

The KC-135A is operated as a public aircraft within the meaning of the Federal Aviation Act of 1958, as amended, and as such does not require or hold a current airworthiness certificate issued by the FAA. The KC-135A is not operated as a common carrier or as a military transport. Consequently, any individual manifested to board the KC-135A should determine before boarding whether his/her personal life or accident insurance provides coverage under such conditions. Also, since the aircraft will be used under test conditions, all test developers and test subjects will be fully informed of the test plans and of all risks, hazards, and discomforts inherent to such tests prior to flight.

Team members are aware that their personal life or accident insurance may not provide coverage while aboard the KC-135A aircraft.

Flight Team:

_____	Date _____
_____	Date _____
_____	Date _____
_____	Date _____

Alternate:

_____	Date _____
-------	------------

Note: Age verification of the Flight Team members are contained in Appendix C.

6. References

Baker, J. and Nayagam, V., 1999, "Buoyancy-Induced Flow in a Non-Uniform Gravity Field," AIAA Paper No. 99-0702.

Kakac, S., Natural Convection, Hemisphere Publishing Corporation (1985)

Holman, J.P., Heat Transfer 8th Edition, McGraw-Hill (1997)

Shigley, Mische, Mechanical Engineering Design 5th Edition, McGraw-Hill (1989)

APPENDIX A - SAMPLE CALCULATIONS

$$\begin{aligned}
 T_1 &:= 300 \text{ K} & \Omega_{\text{RPM}} &:= 50 & v &:= 20.710^{-6} \frac{\text{m}^2}{\text{s}} & U_h &:= 5.0 \cdot 10^{-6} \cdot \text{m} \\
 T_2 &:= 400 \text{ K} & h &:= 0.0508 \text{ m} & & & U_{\Omega_{\text{RPM}}} &:= 0.5 \\
 T_{\text{avg}} &:= \frac{T_1 + T_2}{2} & T_{\text{avg}} &= 350 \text{ K} & \alpha &:= 0.298310^{-4} \frac{\text{m}^2}{\text{s}} & U_{\Omega} &:= \frac{\pi \cdot U_{\Omega_{\text{RPM}}} \cdot 1}{30 \cdot \text{s}} \\
 \beta &:= \frac{1}{T_{\text{avg}}} & \beta &= 2.857 \cdot 10^{-3} \cdot \text{K}^{-1} & U_T &:= 1 \text{ K} & U_{\Omega} &= 0.052 \text{ s}^{-1} \\
 dT &:= T_2 - T_1 & dT &= 100 \text{ K} & & & U_{dT} &:= \sqrt{2 \cdot U_T^2} \\
 \Omega &:= \frac{\pi \cdot \Omega_{\text{RPM}} \cdot 1}{30 \cdot \text{s}} & \Omega &= 5.236 \text{ s}^{-1} & & & U_{dT} &= 1.414 \text{ K}
 \end{aligned}$$

Evaluation of Expression for N2

$$N_2(h, \Omega, dT) := \frac{\beta \cdot dT \cdot h^4 \cdot \Omega^2}{v \cdot \alpha} \quad N_2(h, \Omega, dT) = 8.448 \cdot 10^4$$

Derivatives

$$\frac{dh(h, \Omega, dT)}{dh} := \frac{d}{dh} N_2(h, \Omega, dT) \quad \frac{dh(h, \Omega, dT)}{dh} = 6.652 \cdot 10^6 \cdot \text{m}^{-1}$$

$$\frac{d\Omega(h, \Omega, dT)}{d\Omega} := \frac{d}{d\Omega} N_2(h, \Omega, dT) \quad \frac{d\Omega(h, \Omega, dT)}{d\Omega} = 3.227 \cdot 10^4 \cdot \text{s}$$

$$\frac{ddT(h, \Omega, dT)}{ddT} := \frac{d}{ddT} N_2(h, \Omega, dT) \quad \frac{ddT(h, \Omega, dT)}{ddT} = 844.813 \text{ K}^{-1}$$

Absolute Uncertainty

$$U_{N2} := \left[\left(\frac{dh(h, \Omega, dT)}{dh} U_h \right)^2 + \left(\frac{d\Omega(h, \Omega, dT)}{d\Omega} U_{\Omega} \right)^2 + \left(\frac{ddT(h, \Omega, dT)}{ddT} U_{dT} \right)^2 \right]^{\frac{1}{2}}$$

$$U_{N2} = 2.07 \cdot 10^3$$

Percentage Uncertainty

$$U_{N_2} := \left[\left(\frac{dh(h, \Omega, dT)}{N_2(h, \Omega, dT)} U_h \right)^2 + \left(\frac{d\Omega(h, \Omega, dT)}{N_2(h, \Omega, dT)} U_\Omega \right)^2 + \left(\frac{ddT(h, \Omega, dT)}{N_2(h, \Omega, dT)} U_{dT} \right)^2 \right]^{\frac{1}{2}}$$

$$U_{N_2} = 0.024$$

$$U_{N_2\text{percentage}} := U_{N_2} \cdot 100 \quad U_{N_2\text{percentage}} = 2.45$$

$$dN_2 := U_{N_2} \cdot N_2(h, \Omega, dT)$$

$$dN_2 = 2.07 \cdot 10^3$$

$$h_{\text{uncertainty}} := \left(\frac{dh(h, \Omega, dT)}{N_2(h, \Omega, dT)} U_h \right)^2 \quad h_{\text{uncertainty}} = 1.55 \cdot 10^{-7}$$

$$\Omega_{\text{uncertainty}} := \left(\frac{d\Omega(h, \Omega, dT)}{N_2(h, \Omega, dT)} U_\Omega \right)^2 \quad \Omega_{\text{uncertainty}} = 4 \cdot 10^{-4}$$

$$dT_{\text{uncertainty}} := \left(\frac{ddT(h, \Omega, dT)}{N_2(h, \Omega, dT)} U_{dT} \right)^2 \quad dT_{\text{uncertainty}} = 2 \cdot 10^{-4}$$

APPENDIX B – UNCERTAINTY ANALYSIS

The uncertainty analysis gives the designers an important advantage on the financial planning of the project. The exponents of each variable are calculated and compared to determine which is larger. The variable with the largest exponent will have the largest effect on the overall equation. This will help the designers decide how the money will be dispersed. This decision will give the designers the ability to spend a substantial amount of money on equipment that is necessary in order for the project to be successful.

Using the data reduction equation, we can find the uncertainty, (u_R) , of R. If we let R be one of the unknown parameters, a function of \mathbf{x} , then

$$R = R(x_1, x_2, \dots, x_n)$$

$$\text{and, } u_R^2 = \left(\frac{\partial R}{\partial x_1}\right)^2 (u_{x_1})^2 + \dots + \left(\frac{\partial R}{\partial x_n}\right)^2 (u_{x_n})^2 \text{ is the uncertainty analysis of R.}$$

By normalizing, we get the equation for the uncertainty magnification factor.

$$\left(\frac{u_R}{R}\right)^2 = \left(\frac{x_1}{R} \frac{\partial R}{\partial x_1}\right)^2 \left(\frac{u_{x_1}}{x_1}\right)^2 + \dots + \left(\frac{x_n}{R} \frac{\partial R}{\partial x_n}\right)^2 \left(\frac{u_{x_n}}{x_n}\right)^2$$

The uncertainty percentage contribution is defined as

$$1 = \left(\frac{u_R}{u_R}\right)^2 = \frac{\left(\frac{\partial R}{\partial x_1}\right)^2}{u_R^2} (u_{x_1})^2 + \dots + \frac{\left(\frac{\partial R}{\partial x_n}\right)^2}{u_R^2} (u_{x_n})^2$$

Three dimensionless parameters were calculated:

$$\text{The Prandtl Number, } P_R = \frac{\mathbf{u}}{\mathbf{a}}$$

$$\text{The Nusselt Number, } N_u = \frac{q_w h}{k\Delta T}$$

$$\text{And an unknown, } N_2 = \frac{\mathbf{b} \Delta T \Omega^2 h^4}{\mathbf{u} \mathbf{a}}$$

Where \mathbf{u} = kinematic viscosity
 \mathbf{a} = thermal diffusivity
 q_w = heat flux
 h = height
 k = thermal conductivity
 ΔT = change in temperature
 \mathbf{b} = volumetric expansion coefficient
 Ω = frequency

We assumed $k, \mathbf{a},$ and \mathbf{u} to be constant.

The equations for the Uncertainty Percentage Contribution and the Uncertainty Magnification Factor for N_u and N_2 were found to be:

N_2 Number :

$$1 = \left(\frac{\Omega^4 \Delta T^2 h^8}{\mathbf{a}^2 \mathbf{u}^2 U_{N_2}^2} \right) (U_b)^2 + \left(\frac{4\mathbf{b}^2 \Omega^2 \Delta T^2 h^8}{\mathbf{a}^2 \mathbf{u}^2 U_{N_2}^2} \right) (U_\Omega)^2 + \left(\frac{\mathbf{b}^2 \Omega^4 h^8}{\mathbf{a}^2 \mathbf{u}^2 U_{N_2}^2} \right) (U_{\Delta T})^2 + \left(\frac{16\mathbf{b}^2 \Omega^4 \Delta T^2 h^6}{\mathbf{a}^2 \mathbf{u}^2 U_{N_2}^2} \right) (U_h)^2$$

$$(U_{N_2}/N_2)^2 = \left(\frac{\Omega^2 \Delta T h^4}{\mathbf{a} \mathbf{u} \mathbf{b}} \right) (U_b)^2 + \left(\frac{4\mathbf{b} \Delta T h^4}{\mathbf{a} \mathbf{u}} \right) (U_\Omega)^2 + \left(\frac{\mathbf{b} \Omega^2 h^4}{\mathbf{a} \mathbf{u} \Delta T} \right) (U_{\Delta T})^2 + \left(\frac{16\mathbf{b} \Omega^2 \Delta T h^2}{\mathbf{a} \mathbf{u}} \right) (U_h)^2$$

Nusselt Number :

$$1 = \left(\frac{h^2}{k^2 \Delta T^2 U_{Nu}^2} \right) (U_{q_w})^2 + \left(\frac{q_w^2}{k^2 \Delta T^2 U_{Nu}^2} \right) (U_h)^2 + \left(\frac{q_w^2 h^2}{k^2 \Delta T^4 U_{Nu}^2} \right) (U_{\Delta T})^2$$

$$(U_{Nu}/Nu)^2 = \left(\frac{h}{k \Delta T q_w} \right) (U_{q_w})^2 + \left(\frac{q_w}{k \Delta T h^2} \right) (U_h)^2 + \left(\frac{h q_w}{k \Delta T^4} \right) (U_{\Delta T})^2$$

The Percent Reduction equation displays the uncertainty percentage each variable contributes to the overall uncertainty of the dimensionless number. Through the comparison of these values, it can be shown which variable is most important to reducing the overall uncertainty of the number. (For example, if q_w contributes 85% of the uncertainty to the Nusselt Number, it would be important to use very precise instruments

when measuring this number in order to reduce this uncertainty, while the h and ΔT could be measured with relatively inexpensive instruments.) The Uncertainty Magnification Factor equation displays the magnitude of uncertainty for each variable. (For example, if q_w has an uncertainty on the order of 10^6 while h and ΔT have an uncertainty on the order of 10^2 , it would be important to measure q_w very precisely to reduce this large uncertainty.) Through this process, these equations can be used to determine how equipment money should be spent.

In the above equations, one can get a very superficial sense of how each variable will affect the uncertainty of the dimensionless numbers. This is achieved by comparing the exponents of a variable for each term. For example, it is seen that h will affect the uncertainty of q_w the same amount as ΔT , in both the percent reduction equation and the magnification factor equation.

APPENDIX C – AGE VERIFICATION

APPENDIX D - FACULTY ENDORSEMENT

APPENDIX E – TEAM ADVISOR

John Baker, Ph.D.

Address

UAB Department of Materials and Mechanical Engineering
358B BEC, 1150 10th Ave S, Birmingham, AL 35294-4461
Phone: (205) 934-7508 Facsimile: (205) 934-8485 (Office)
E-mail: jbaker@eng.uab.edu

Education

1993 Ph.D. University of Kentucky; Lexington, Kentucky
1990 MSME University of Kentucky; Lexington, Kentucky
1987 BSME University of Kentucky; Lexington, Kentucky

Professional Experience

1/94- Assistant Professor, Department of Materials and Mechanical Engineering
University of Alabama at Birmingham; Birmingham, Alabama
11/98- Director, UAB Mechanical Engineering Undergraduate Laboratories
University of Alabama at Birmingham; Birmingham, Alabama
3/96-3/97 Director, UAB Mechanical Engineering Graduate Program
University of Alabama at Birmingham; Birmingham, Alabama
6/93-9/93 Guest Student, Department of Physical Oceanography
Woods Hole Oceanographic Institution; Woods Hole, Massachusetts
6/92-8/92 Instructor, Department of Mechanical Engineering
University of Kentucky; Lexington, Kentucky
8/91-5/92 Teaching Assistant, Department of Mechanical Engineering
University of Kentucky; Lexington, Kentucky
6/91-8/91 Instructor, Department of Mechanical Engineering
University of Kentucky; Lexington, Kentucky
9/90-11/91 Research Engineer
Cudo Technologies, Ltd, Lexington, Kentucky
6/90-8/90 Instructor, Department of Mechanical Engineering
University of Kentucky; Lexington, Kentucky
1/89-5/90 Teaching Assistant, Department of Mechanical Engineering
University of Kentucky; Lexington, Kentucky
6/89-9/89 Research Associate, AFOSR/UES Graduate Student Research Program
Computational Aerodynamics Group, Wright-Patterson Air Force Base, Ohio

Awards and Honors

1998 Finalist, Ingalls-UAB National Alumni Excellence in Classroom Teaching Award,
1997-99 UAB Faculty Senator (School of Engineering Representative)
1997 Finalist, Ingalls-UAB National Alumni Excellence in Classroom Teaching Award
1997 UAB President's Excellence in Teaching Award (Engineering)
1991 "Best Paper" in Hypersonics Award
AIAA 17th Annual Mini-Symposium on Aerospace Science and Technology; Dayton,
Ohio

Honorary Societies:

- Tau Beta Pi (national engineering honorary)
- Pi Tau Sigma (mechanical engineering honorary)
- Phi Theta Kappa (national junior college honorary)

Selected Publications

1. Prasad, K. and Baker, J., 1999, "Nucleate Pool Boiling Over a Vertical Steps," accepted for publication, *J. Thermophy. and Heat Trans.*
2. Baker, J., 1999, "Thermal Radiation and Natural Convection In A Non-Uniform Artificial Gravity Field," AIAA Paper No. 99-3743.
3. Calvert, M.E. and Baker, J., 1999, "Heat Transfer and Para/Diamagnetic Jets: A Computational Investigation," AIAA Paper No. 99-3742.
4. Baker, J., Ponnappan, P., and Leland, J., 1999, "Rotating Heat Pipe: A Computational Investigation Into Performance Characteristics," AIAA Paper No. 99-3444.
5. Baker, J. and Saito, K., 1999, "Magnetic Fields And Equilibrium Combustion Characteristics," AIAA Paper No. 99-3751.
6. Gao, P., Dillon, H.K., Baker, J., and Oestestad, K., 1999, "Numerical Prediction Of The Performance Of A Manifold Sampler With A Circular Slit Inlet In Turbulent Flow," *J. Aerosol Sci*, Vol.30, No.3, pp.299-312.
7. Baker, J. and Nayagam, V., 1999, "Buoyancy-Induced Flow in a Non-Uniform Gravity Field," AIAA Paper No. 99-0702.
8. Calvert, M.E. and Baker, J., 1999, "Flow Field Characteristics of a Parametric Jet in the Presence of a Non-Uniform Magnetic Field," AIAA Paper No. 99-0678.
9. Baker, J., Ponnappan, P., and Leland, J., 1999, "A Computational Model of Transport within a Rotating Heat Pipe," AIAA Paper No. 99-1070.
10. Calvert, M.E. and Baker, J., 1998, "Thermal Conductivity and Gaseous Microscale Transport," *J. Thermophy. & Heat Trans.*, Vol. 12, No. 2, pp.138-145.
11. Ponnappan, R., He, Q., Baker, J., Myers, J.M., and Leland, J., 1997, "High Speed Rotating Heat Pipe: Analysis and Test Results," 10th International Heat Pipe Conference, Stuttgart, Germany, September 22-26.
12. Baker, J. and Calvert, M.E., 1997, "Micro-Scale Transport: Non-Continuum Thermophysical Property Variation Effects on Heat and Momentum Transfer," AIAA Paper No. 97-0377.
13. Baker, J., 1996, "Thermal Radiation and the Thermal Management of Micro-Devices Via Gaseous Flows," in *Proceedings of the ASME AES Div.*, 1996 ASME-IMECE, AES-Vol. 36, pp. 31-37.
14. Baker, J., Calvert, M.E., Power, D.J, Chen, E.T., Ramalingam, M.L., and Lamp, T.R., 1996, "On the Role of the Knudsen Number with Respect to Heat Transfer in Micro-Scale Flows," Paper No. 96135, 31st IECEC, Washington, D.C.
15. Baker, J. and Calvert, M.E., 1996, "Effect Of Variable Viscosity On Coupled Heat And Momentum Transfer In Microchannel Flows," in *Proceedings of the Fluids Engineering Division Summer Meeting - 1996*, FED-Vol. 237, pp.775-782.
16. Trant, T.E. and Baker, J., 1996, "On the Use of Chaotic Maps to Model the Small-Scale Flow Behavior for the Study of Planetary Boundary Layer Turbulence," AIAA Paper No.96-0393.
17. Baker, J. and Trant, T.E., 1995, "On the Use of Chaotic Maps to Model the Small-Scale Flow Structure in an Additive Turbulent Decomposition of Burgers Equation," in *Proceedings of the ASME Fluids Engineering Division*, 1995 ASME-IMECE, FED-Vol. 234, pp. 269-276.
18. Baker, J., Singh, S.N. and Saito, K., 1993c, "Thermal Stability of Two, Horizontal Fluid Layer with Radiative Heating from Above," in *Fundamentals of Natural Convection 1993*, 1993 ASME-WAM, HTD-Vol.264, pp.17-30.